



Cite this: *RSC Adv.*, 2025, 15, 875

# The coiled-coil protein carrier structure affects the activation of certain endocytosis pathways†

Ken-Ichi Sano <sup>\*ab</sup> and Yuta Nomata<sup>b</sup>

Coiled-coil protein carrier (CCPC) 140 is a rigid and anisotropically structured cationic coiled-coil artificial protein that has displayed up to a 1000 times higher level of cellular internalization activity than that of unstructured cell-penetrating peptides. Previous studies have demonstrated that CCPC 140's rigid and anisotropic structural properties and cationic surface properties are important for its superior cellular internalization activity. In this study, we investigated whether each physicochemical characteristic of CCPC 140 effectively contributed to activating the cellular internalization pathway. By evaluating CCPC 140's ability to penetrate glycosaminoglycan (GAG)-lacking cells, the activation of GAG-dependent endocytosis by electrostatic interactions between cationic CCPC 140 and anionic GAGs has been found to play a major role in CCPC 140's superior cellular internalization activity. Using endocytosis inhibitors, it was revealed that the GAG-binding-dependent activation of caveola-mediated endocytosis plays a role in cellular internalization, which requires rigid and anisotropic structural properties, not the cationic properties of CCPC 140. Macropinocytosis is a common route of cellular internalization. However, CCPC 140's rigid and anisotropic structural properties activate macropinocytosis, but this does not involve the Rho-family GTPase-dependent macropinocytosis pathway.

Received 31st October 2024

Accepted 7th January 2025

DOI: 10.1039/d4ra07763f

rsc.li/rsc-advances

## 1 Introduction

The efficient intracellular delivery of therapeutic molecules using peptides has been achieved by mimicking viral infections. The first cell-penetrating peptide (CPP) was found in the human immunodeficiency virus TAT protein.<sup>1,2</sup> Heretofore, considerable variations in CPPs have been detected in natural proteins, and artificial peptides have been designed to exhibit cell-penetrating activity.<sup>3–5</sup> Most CPPs are highly cationic because inter-ionic interactions between the positively charged CPPs and the negatively charged proteoglycans and phospholipids of the plasma membrane's extracellular domains are thought to be important for cellular internalization.<sup>6–9</sup>

In particular, the binding of glycosaminoglycans (GAGs) to proteoglycans has been reported as a trigger for the internalization of most CPPs by endocytosis.<sup>3,6–14</sup> CPPs, such as Tat and oligo-arginine, exhibit largely decreasing cellular internalization activity against the Chinese hamster ovary (CHO)-derived *pgsA*-745 cell line, which lacks GAGs on its cell surface.<sup>10–13</sup>

The cellular internalization of CPPs is not limited to endocytosis, but can also occur through direct penetration, that is, translocation.<sup>6–9,15,16</sup> However, most CPPs show a dramatic reduction in the extent of cell penetration when endocytosis is suppressed.<sup>13,15–19</sup> These studies indicate that GAG-dependent endocytosis is the most effective pathway of intracellular delivery using CPPs. However, high concentrations of CPPs, in most cases 5–10  $\mu$ M, are required for endocytic activation. The requirement for the high concentration and cooperative cellular internalization of CPPs is explained by the accumulation and formation of clusters on GAGs, which trigger the activation of endocytosis.<sup>6,8,20</sup>

Asbestos and carbon nanotubes, being rigid and anisotropic (fibrous) nanomaterials, show remarkably effective cellular internalization.<sup>21–23</sup> However, they are highly toxic in the long term because of their non-biodegradability.<sup>21,24–26</sup> In a previous study, we hypothesized that an artificial protein having a highly cationic surface and rigid and anisotropic structure would show superior cellular internalization activity.<sup>27</sup> Long-term toxicity should have been avoided since the protein was biodegradable. Therefore, we designed and produced an artificial protein, coiled-coil protein carrier (CCPC) 140 ("140" refers to the number of amino acid residues in the polypeptide chain of CCPC. Fig. 1A), with a structured frame derived from the filamentous protein tropomyosin, the entire molecule of which consists of a two-stranded parallel  $\alpha$ -helical coiled-coil structure.<sup>27</sup> Similar to tropomyosin, CCPC 140 has an anisotropic structure, with a 2 nm diameter and 20 nm length (Fig. 1B).<sup>27–30</sup>

<sup>a</sup>Department of Applied Chemistry, Faculty of Fundamental Engineering, Nippon Institute of Technology, 4-1 Gakuidai, Miyashiro, Saitama 345-8501, Japan. E-mail: kisano@nit.ac.jp

<sup>b</sup>Graduate School of Environmental Symbiotic System Major, Nippon Institute of Technology, 4-1 Gakuidai, Miyashiro, Saitama 345-8501, Japan

† Electronic supplementary information (ESI) available: Fig. S1: microscopic observations of the cellular internalization of CCPCs. Fig. S2: cytotoxicity of endocytic inhibitors using in this study. See DOI: <https://doi.org/10.1039/d4ra07763f>



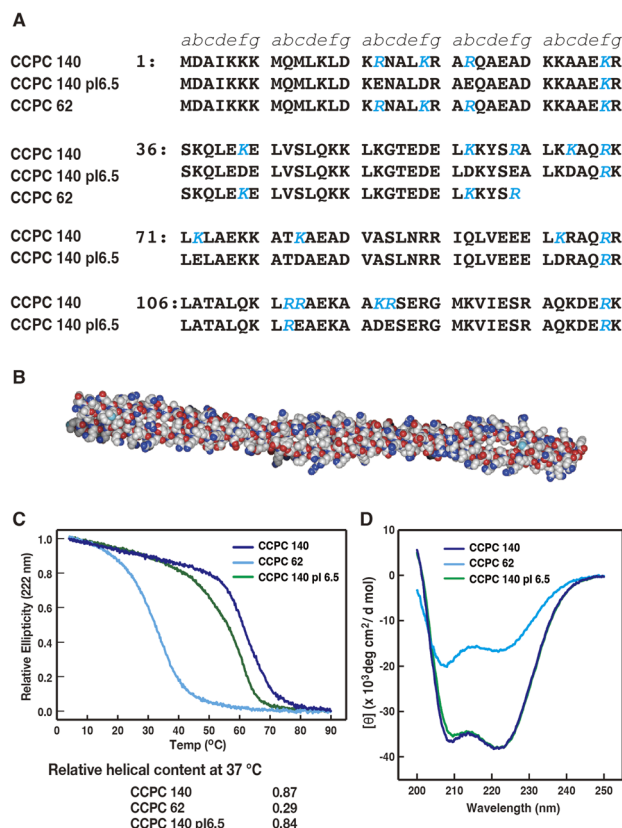


**Fig. 1** (A) Amino acid sequence of CCPC 140, CCPC 140 pI 6.5 and CCPC 62 (adapted with permission from ref. 34. Copyright 2015 American Chemical Society). The positions of the heptad repeat are described as *a* to *g*. Letters in blue represent substituted amino acids from human skeletal muscle  $\alpha$ -tropomyosin. (B) Designation of CCPC 140 using the SWISS-MODEL Repository,<sup>28,29</sup> and drowned space-filling model using Waals (Altif Laboratories, Tokyo, Japan). (C) Thermal unfolding profiles of CCPC 140, CCPC 140 pI 6.5, and CCPC 62. Relative helical contents are calculated as shown in the Materials and methods. (D) Circular dichroism spectra of CCPC 140, CCPC 140 pI 6.5, and CCPC 62 at 37 °C.

The  $\alpha$ -helical coiled-coil primary structure shows a heptad-repeat amino acid sequence with each position assigned *a* to *g*. The amino acids at positions *b*, *c*, and *f* are exposed outside the coiled-coil structure, and these amino acids define the surface properties of coiled-coil proteins.<sup>31,32</sup> CCPC 140 was designed to have 53.3% basic amino acids, lysine and arginine at positions *b*, *c*, and *f*, and a calculated isoelectric point of 10.6.<sup>27</sup> Thus, the surface of CCPC 140 was highly cationic. Physicochemical studies on tropomyosin have revealed that its persistence length is presumed to be longer than its actual length.<sup>33</sup> This accounts for the rigid and anisotropic structure of CCPC 140.

Investigating the cellular internalization activity of fluorescently labeled CCPC 140 against several tumor-derived human cell lines, such as HeLa cells, Hep3B, A549, and K562, showed its superior cellular internalization.<sup>27</sup> Regarding the HeLa cells, CCPC 140 was detected in all cells at a concentration as low as 3.1 nM.<sup>27</sup> Higher concentrations are usually required

for the internalization of CPPs by endocytosis, as described above.<sup>6–15</sup> This indicates that the cellular internalization activity of cationic, rigid, and anisotropically structured CCPC 140 was approximately 1000 times greater than that of cationic but unstructured CPPs.<sup>27</sup> Due to the high cellular internalization activity of CCPC 140, it may reduce the administered concentration of anticancer drugs with IC<sub>50</sub>s in the tens of  $\mu$ M range (unpublished result).

We also created CCPC 140 variants with noncationic surfaces. Their isoelectric points were 6.5 and 8.6, named CCPC 140 pI 6.5 and CCPC 140 pI 8.6, respectively.<sup>34</sup> Compared to CCPC 140, a 100 times higher concentration of the CCPC 140 pI variants was required for cellular internalization.<sup>34</sup> We also evaluated the effect of the structural rigidity of CCPC 140 on cellular internalization.<sup>27</sup> A deletion variant of CCPC 62 having 62 amino acids per chain could not maintain its coiled-coil structure at 37 °C, the experimental temperature of a cellular internalization assay, because of thermal fluctuation.<sup>27</sup> The cellular internalization activity of CCPC 62 is much lower than that of CCPC 140.<sup>27,35</sup> At the effective concentration, the activity of CCPC 62 is slightly superior but almost comparable to that of other CPPs.<sup>27</sup> In contrast, LZ-CCPC 62, a CCPC 62 variant with the same number of positively charged residues at the same positions, has an  $\alpha$ -helical coiled-coil structure formation at 37 °C; it exhibits cellular internalization activity equal to that of CCPC 140.<sup>35</sup> From the study of a series of deletion variants of LZ-CCPCs, an aspect ratio at 4.5 : 1 or more was required for the superior cellular internalization of the cationic coiled-coil proteins.<sup>35</sup>

Thus, we addressed the factors necessary for the superior cellular internalization of CCPC 140 based on the physicochemical properties of the molecule. Although the subcellular localization of DDS carriers is a critical issue in intracellular DDS research, that of CCPC 140 is still unknown. Previous studies have shown that the mechanism underlying the superior cellular internalization activity of CCPC 140 relies on the activation of endocytosis, but the details of this are unclear.<sup>27</sup> This work, however, focuses on the first step of CCPC 140 entry into the cell. We clarified the endocytic pathways activated by each physicochemical property, including the rigid and anisotropic structural properties and cationic surface properties, of CCPC 140.

## 2 Materials and methods

### 2.1. Preparation of CCPC 140 and its derivatives

The preparation of CCPC 140 and its derivatives has been described in our previous reports.<sup>27,34,35</sup> Purified CCPC 140 and its derivatives were checked by SDS-PAGE. Protein concentrations were determined using the micro-burette method.<sup>36</sup>

### 2.2. Circular dichroism measurements

Thermal denaturation of the protein was evaluated using a JASCO J-820 circular dichroism (CD) spectropolarimeter equipped with a CTU-100 Peltier temperature controller. The sample was placed in a 1 mm quartz cuvette. Temperature-



dependent CD values and far-UV CD spectra were obtained as previously described.<sup>35</sup> The relative helical content of the CCPC 140 and CCPC variants was evaluated with the following equation:

$$\text{Relative helical content} = \frac{([\theta]_{222 \text{ nm}}]_{\text{temp}} - [\theta]_{222 \text{ nm}}]_{4 \text{ }^{\circ}\text{C}}}{([\theta]_{222 \text{ nm}}]_{90 \text{ }^{\circ}\text{C}} - [\theta]_{222 \text{ nm}}]_{4 \text{ }^{\circ}\text{C}}}$$

### 2.3. *In vitro* cell penetration assay

CCPC 140 and its derivatives were labeled with Alexa Fluor 532 (Life Technologies, California, USA) as previously described.<sup>35</sup> Labeled CCPC protein concentrations were determined using the micro-burette method,<sup>36</sup> and the concentration of the conjugated Alexa Fluor 532 dye was determined at an absorbance of 532 nm. Then, the efficiency of the fluorescently labeled recombinant proteins was estimated by their division.

*In vitro* cell penetration assays were carried out according to our previous reports.<sup>35</sup> In brief, two CHO cell lines, CHO-K1 (JCRB cell bank JCRB9018) and *pgsA-745* (ATCC CRL-2242),<sup>37</sup> were used in this study and were obtained from the JCRB cell bank and ATCC, respectively. Both cell lines used for the assays had a passage number less than 15. The cells were maintained in Ham's F-12 nutrient mix medium (Gibco, Thermo Fisher) supplemented with 10% fetal calf serum (FCS) and penicillin-streptomycin (Wako-Fujifilm) at 37 °C under humidification with 5% CO<sub>2</sub>-containing air.

For the cell penetration assay, the cells were plated at a density of  $5 \times 10^4$  cells per well in a 24-well plate. After 16–20 h incubation, the medium was replaced with 500 µl of Ham's F-12 nutrient mix medium supplemented with 10% FCS, penicillin-streptomycin, and fluorescently labeled CCPC 140 and its derivatives and incubated for 2 h. The inhibitors nystatin, jasplakinolide, and toxin B were added at final concentrations of 50 µg mL<sup>-1</sup>, 10 ng mL<sup>-1</sup>, and 50 nM, respectively. Neuraminidase was added at a final concentration of 50 mU mL<sup>-1</sup> 30 min prior to addition of CCPC 140 and its derivatives. The effect of both CCPCs and these inhibitors on the cell proliferation was assessed by the WST-1 [4-[3-(4-iodophenyl)-2-(4-nitrophenyl)-2H-5-tetra-zolio]-1,3-benzene disulfonate] (Takara, Japan) assay. CCPCs and Inhibitors were added at the same concentration as that used in the cell penetration assay. The cells were then incubated for 2 h and assayed using a WST-1 kit.

For the fluorescence-activated cell sorting (FACS) assay, the cells were treated with 500 µl of 0.25% w/v Trypsin-1 mM EDTA-4Na (Wako-Fujifilm) and incubated for 1–2 min; the trypsin solution was removed, and protease activity was stopped by the addition of 500 µl of Ham's F-12 nutrient mix medium supplemented with 10% FCS. The cells were detached from the 24-well plate by gentle pipetting and collected by centrifugation at 1500g for 2 min at 20–25 °C. The cells were washed twice with 500 µl of PBS and suspended in 200 µl of PBS, and the fluorescent intensity from each cell was measured using a FACS Moxiflow instrument (ORFLO, Ketchum, Idaho, USA).

For microscopic observation, after two hours of incubation of fluorescently labeled CCPC 140 and its derivatives in the medium, the cells were washed twice with 500 µl PBS, and 500 µl DMEM/F-12 nutrient mixture medium (Gibco) without

phenol red and supplemented with 10% FCS was added. The cells were observed using an Evos M5000 imaging system (Thermo Fisher Scientific).

## 3 Results and discussion

### 3.1. Evaluation of structural stability of CCPC 140 and its variants

First, we obtained the thermal denaturation profiles and CD far-UV spectra at a cell-penetration experimental temperature of 37 °C for CCPC 140 and its derivatives using CD spectroscopy (Fig. 1C and D). The results agreed with those of our previous studies.<sup>27,34</sup> The thermal melting profiles revealed that CCPC 140 and CCPC 140 pI 6.5 still maintained a high  $\alpha$ -helical content at 37 °C (0.87 and 0.84, respectively), but the structure of CCPC 62 was almost lost (0.29) because of thermal fluctuation. The far-UV CD spectra profiles of CCPC 140 and CCPC 140 pI 6.5 also demonstrate the maintenance of their  $\alpha$ -helical coiled-coil structure at the experimental temperature. In conclusion, both CCPC 140 and CCPC 140 pI 6.5 displayed a rigid and anisotropic structure during the cell penetration assay, and CCPC 62 did not form a coiled-coil structure but did form a partially folded  $\alpha$ -helix.

### 3.2. Effect of GAGs on the cellular internalization activities of CCPC 140 and its variants

The binding to GAGs of proteoglycans has been shown to trigger CPPs and viral internalization by endocytosis. We investigated the effect of GAG binding on CCPC 140 and its variant cellular internalization activities (Fig. 2–4). The CHO-derived *pgsA-745* strain lacks GAGs<sup>37,38</sup> and is often used to evaluate the GAG-binding-triggered cell penetration of CPPs and viruses.<sup>10–13,39–41</sup> To compare the cellular internalization activity of CCPC 140, uncationic CCPC 140 pI 6.5, and partially folded CCPC 62, we evaluated the effect of both the electrostatic interactions between CCPCs and GAGs and the structural rigidity and anisotropy of CCPCs on cellular internalization.

CCPC 140 and its derivatives were fluorescently labeled with Alexa Fluor 532. The labeled CCPC 140 and its derivatives were adjusted to a molar ratio of 1.8–2.1 (two polypeptide chains reduced to one molecule), which was confirmed by the protein concentration and fluorophore absorbance. One possible effect on CCPC molecule by labeling is a decrease in primary amine at the surface of CCPCs (mainly side chain of lysine). This can cause decreasing *pI* of CCPCs. To minimize the effect of labeling on CCPCs structure and functions, almost one fluorophores bound on each CCPC polypeptide chain. The labeled CCPC 140 and its derivatives were added to both wild-type CHO-K1 with GAGs and *pgsA-745* cultures at concentrations ranging from 10 nM to 1 µM, and the cellular uptake of the labeled CCPC 140 and its derivatives was examined using fluorescence microscopy and FACS (Fig. 2, 3 and S1†). Generally, cationic polymers are known to show cytotoxicity concentration dependent manner, we have confirmed that no significant cytotoxicity was observed at the concentrations of CCPCs used in this study (Fig. S2†). We detected a significant fluorescence signal from the cells 2 h after



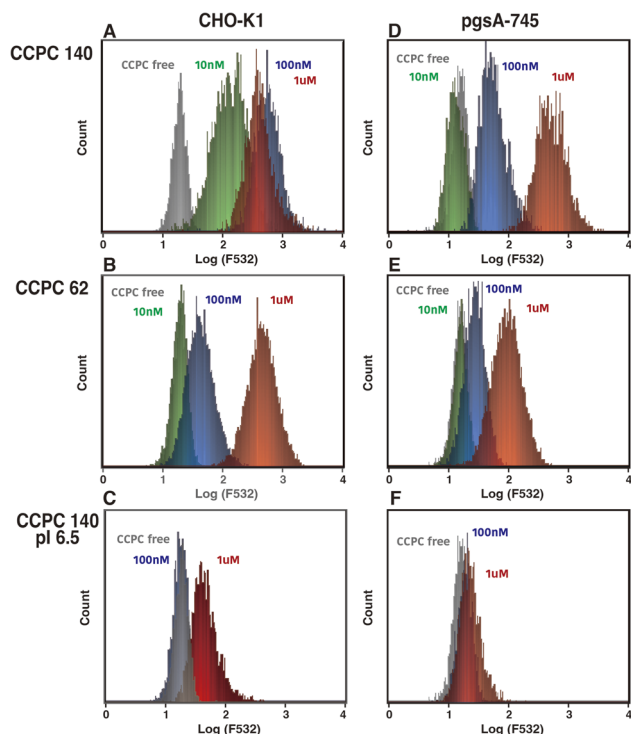


Fig. 2 Quantitative FACS analysis of the cell-penetrating activity of Alexa Fluor 532-labeled CCPCs against CHO-K1 (A–C) and *pgsA-745* (D–F). (A and D) are CCPC 140, (B and E) are CCPC 62, and (C and F) are CCPC 140 pl 6.5 administrated cells, respectively. Cells were incubated without CCPCs (gray) and with 10 nM (green), 100 nM (blue) and 1  $\mu$ M (red). Fluorescent labeling efficiency is 1.8, 2.0, and 2.0 for CCPC 140, CCPC 140 pl 6.5, and CCPC 62, respectively.

we added CCPC 140 to CHO-K1 cells at a final concentration of 10 nM (Fig. 2, S1,† and 4A). These observations agree with those made in our previous experiments using human cancer-derived cell lines.<sup>27</sup> The FACS data showed that the fluorescent signals from each cell were saturated with more than 100 nM CCPC 140 in the CHO-K1 cells (Fig. 3A). Although we did not detect significant fluorescence signals from *pgsA-745* at 10 nM CCPC

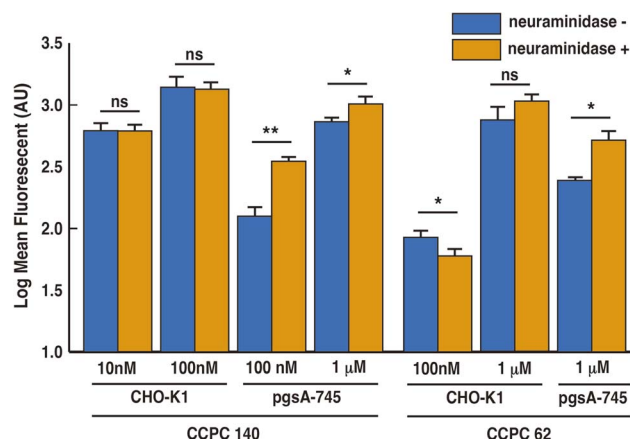


Fig. 4 Mean fluorescence intensities of quantitative FACS analysis of the cell-penetrating activity of Alexa Fluor 532-labeled CCPCs against CHO-K1 and *pgsA-745* with (orange) or without (blue) neuraminidase treatment. Fluorescent label efficiency is 2.1 and 2.0 for CCPC 140 and CCPC 62, respectively. Data from four independent measurements were averaged. The error bar represents the standard error. \* means  $P < 0.05$ ; \*\* means  $P < 0.005$  for neraminidase untreated CCPC-interalized cells.

140, 100 nM and 1  $\mu$ M CCPC 140 were sufficient to detect significant fluorescence signals from *pgsA-745* (Fig. 4A). This tendency was also seen in the partially folded but cationic CCPC 62 (Fig. 3B). The cellular internalization activity of CCPC 62 was much lower than that of CCPC 140 but was also affected by the GAGs. These results agree with previous reports using unstructured but cationic CPPs.<sup>12–15</sup> In the case of the structured but noncationic CCPC 140 pl 6.5, significant fluorescent signals were detected only with 1  $\mu$ M addition to CHO-K1 (Fig. 3C).

These results show that the activation of GAG-dependent endocytosis plays a major role in the superior cellular internalization activity of CCPC 140, similar to CPP cell penetration. Moreover, as indicated by previous studies, this activation occurs through electrostatic interactions between the cationic CCPCs and acidic GAGs. However, the rigid and anisotropic structural properties of CCPC 140 can enhance the induction

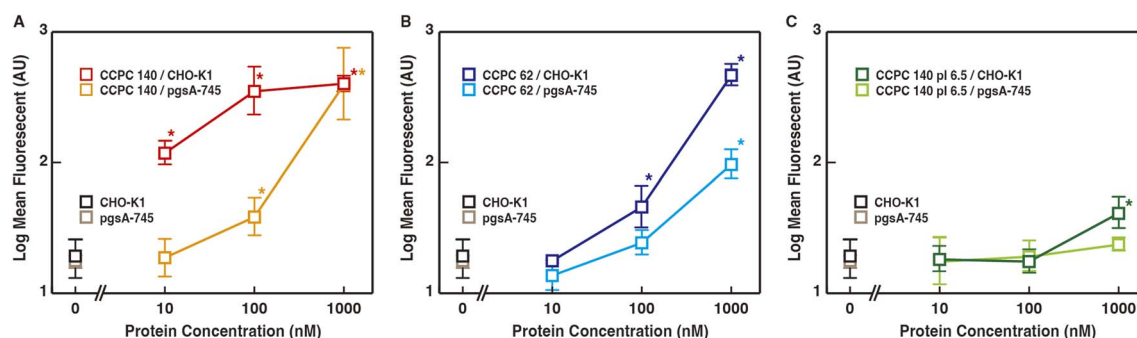


Fig. 3 Mean fluorescence intensities of quantitative FACS analysis of the cell-penetrating activity of Alexa Fluor 532-labeled CCPCs against CHO-K1 and *pgsA-745*. (A) CCPC 140 administrated CHO-K1 (red) and *pgsA-745* (orange). (B) CCPC 62 administrated CHO-K1 (purple) and *pgsA-745* (light blue). (C) CCPC 140 pl 6.5 administrated CHO-K1 (green) and *pgsA-745* (yellow-green). Fluorescent labeling efficiency is 1.8, 2.0, and 2.0 for CCPC 140, CCPC 140 pl 6.5, and CCPC 62, respectively. Three independent measurements were averaged. The error bar represents the standard error. \* means  $P < 0.05$  against untreated cells.





of GAG-dependent endocytosis to a much larger extent than those of unstructured cationic CPPs and partially folded CCPC 62. CPPs and CCPC 62, accumulation and cluster formation on GAGs are required to activate GAGs-dependent endocytosis.<sup>6,8,20</sup> On the other hand, the activation of GAGs-dependent endocytosis by CCPC 140 would require only a few molecules at most.

Interestingly, adding 1  $\mu$ M CCPC 140 to *pgsA-745* allowed cellular internalization to reach the saturation level of the fluorescence signal. For CCPC 140 at a high concentration (1  $\mu$ M), CCPC 140-activated GAG-independent endocytosis can compensate for the loss of GAG-dependent endocytosis. Sialic acid and hyaluronan binding-mediated endocytosis are considered candidates for GAG-independent endocytosis.<sup>12,15,42</sup>

### 3.3. Effect of neuraminidase treatment on the cellular internalization activities of CCPC 140 and its variants

Previous studies showed that the cellular internalization activity of unstructured CPPs was reduced by the removal of sialic acid from cell surfaces.<sup>12,15</sup> Neuraminidase catalyses the hydrolysis of sialic acid. To evaluate the effect of sialic acid binding on the cellular internalization of CCPC 140 and CCPC 62, we investigated the effect of sialic acid removal on the cellular internalization ability of CCPCs (Fig. 4).

We found a significant increase in the cellular internalization activity by adding CCPC 140 and CCPC 62 to *pgsA-745* cells with neuraminidase treatment. In the absence of GAGs on the cellular surface, sialic acid seems to display an inhibitory potency against both structured and partially folded CCPCs. On the other hand, in the presence of GAGs, the neuraminidase treatment had no effect on the cellular internalization activity of CCPC 140, whereas an inhibitory effect was observed on the cellular internalization activity of CCPC 62 (Fig. 4). Sialic acid itself has an inhibitory effect on the cellular internalization activity, but for unstructured CPPs and partially folded CCPC 62, it may act to recruit CPPs to GAGs due to its acidic properties. Also, it was found that the binding of CCPC 140 to GAGs does not require the recruitment by sialic acid because of its structural properties.

### 3.4. Cellular internalization mechanisms of CCPC 140 and its variants

There was considerable variation in the activation of endocytic pathways. Previous CPP studies have indicated that CPPs activate multiple endocytosis pathways through many routes and can penetrate cells. Using endocytosis inhibitors, we attempted to clarify which endocytic pathways were activated by each physicochemical characteristic of CCPC 140. We refer to the experimental conditions used to measure the significant fluorescent signals in Fig. 3, and also evaluate the cellular internalization activities using FACS (Fig. 5). We have confirmed that there the endocytosis inhibitors had no effect on the cell viability under the conditions of the current experiment (Fig. S3†).

Endocytic pathways include various mechanisms involving endocytosis and macropinocytosis. Nystatin breaks lipid raft

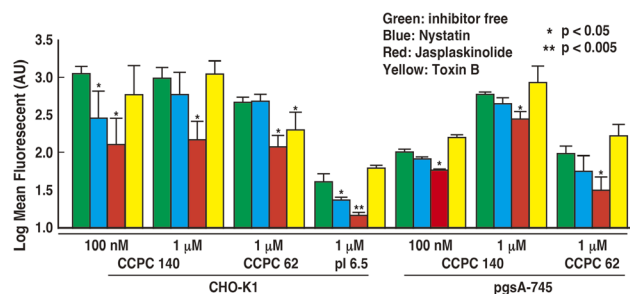


Fig. 5 Mean fluorescence intensities of quantitative FACS analysis of the cell-penetrating activity of Alexa Fluor 532-labeled CCPCs against CHO-K1 and *pgsA-745* with nystatin (blue), jasplakinolide (red) and toxin B (yellow) or without endocytosis inhibitors (blue) without endocytosis inhibitors. Data from three independent measurements were averaged. Fluorescent label efficiency is 2.1, 2.0, and 2.0 for CCPC 140, CCPC 140 pI 6.5, and CCPC 62, respectively. The error bar represents the standard error. \* means  $P < 0.05$ ; \*\* means  $P < 0.005$  for inhibitor-free CCPC-penetrated cells.

structures and abolishes membrane raft endocytosis.<sup>43–46</sup> Thus, nystatin acts as an inhibitor of caveola-mediated endocytosis. CCPC 140 and CCPC 140 pI 6.5 displayed significantly decreased cellular internalization of CHO-K1 cells with the addition of nystatin (Fig. 5). This decrease in the cellular internalization activity of CCPC 140 was not observed at a concentration of 1  $\mu$ M. It was also not observed when CCPC 140 was administrated to GAG-free *pgsA-745* cells. In contrast, the cellular internalization activity of partially folded CCPC 62 was not significantly affected with either CHO-K1 or *pgsA-745* cells (Fig. 5).

On one hand, macropinocytosis often plays a much more important role in the cellular internalization of CPPs than endocytosis does.<sup>6–8,11–13</sup> Jasplakinolide is known to completely inhibit macropinocytosis by inhibiting actin cytoskeleton reconstitution.<sup>47,48</sup> Jasplakinolide inhibited the cellular internalization activity of CCPC 140 and its variants under all the conditions tested in our experiments (Fig. 5). Toxin B also inhibits macropinocytosis through the inhibition of Rho family GTPase activity.<sup>49,50</sup> The cellular internalization ability of CCPC 62 with CHO-K1 cells appeared to be affected by the addition of toxin B (Fig. 5). This decrease in the cellular internalization activity of CCPC 62 was not observed with *pgsA-745* cells. In contrast, the cellular internalization activity of CCPC 140 and CCPC 140 pI 6.5 was unaffected by toxin B in CHO-K1 and *pgsA-745* cells (Fig. 5).

The cellular internalization pathway of CCPC 140 seems to involve macropinocytosis more than caveolae endocytosis when comparing the degree of inhibition of cellular internalization activity of CCPC 140. In addition, macropinocytosis is a common route for the cellular internalization of CPPs, CCPC 140, and its variants.<sup>6–8,11–13</sup> Previous studies have shown that CPPs binding to proteoglycans, including cell-surface GAGs, trigger the activation of Rac1, a Rho family GTPase.<sup>13,51</sup> Following actin remodeling induced by Rac1, CPPs are internalized into cells through macropinocytosis.<sup>13,51</sup> Although structured and partially folded CCPCs are internalized through



macropinocytosis, the signaling pathway leading to actin remodeling activation differs from that associated with structured CCPCs and partially folded CCPC 62 (Fig. 6). The rigid and anisotropic structures of CCPCs, CCPC 140, and CCPC 140 pI 6.5 do not significantly affect the activation of Rho family GTPase-dependent macropinocytosis. In addition, the activation of macropinocytosis by the structured CCPCs does not seem to depend on the interaction between the cationic surface of CCPC 140 and GAGs.

It has been reported that unstructured short CPPs, such as octa-arginine and TAT, do not effect cellular internalization with the addition of nystatin.<sup>11,45,46</sup> Nystatin's effect on the cellular internalization of CCPC 140 was only seen when 100 nM CCPC 140 was administered to CHO-K1 cells (Fig. 5). At higher concentrations (1  $\mu$ M), nystatin's effect was not seen, possibly because the other endocytic pathways activated by CCPC 140 can be fully compensate nystatin's effect. However, this does not mean that the caveolae endocytosis pathway is not important for the cellular internalization of CCPC 140. The caveolae endocytosis pathway can be an important endocytic pathway at low concentrations of CCPC 140. The most significant feature of CCPC 140 is its ability to internalize cells efficiently, even when administered at low concentrations.

It has also been reported that proline-rich CPPs use caveola-mediated endocytosis for internalization.<sup>52</sup> Proline-rich CPPs tend to form fibrillar structures by self-assembly.<sup>52</sup> Therefore, we speculate that caveola-mediated endocytosis is a common route for the cellular internalization of both fibrillar proline-rich CPPs and CCPC 140. Furthermore, CPP-cargo protein conjugates and a PepFact14/DNA conjugate displayed cellular internalization *via* caveolae endocytosis.<sup>18,19,53–55</sup> In the PepFact14/DNA conjugate, a tightly formed peptide/DNA polyanion complex might work as a structural factor for the activation of caveola-mediated endocytosis.<sup>50</sup> In the case of CPP-cargo protein conjugates, a portion of the cargo protein also becomes a factor for activating caveola-mediated endocytosis.<sup>18,19,53,54</sup> Thus, we consider that low-concentration CCPC 140-activated GAG-binding-dependent activation of caveola-mediated endocytosis is due to the anisotropic structure of CCPC 140 (Fig. 6).<sup>53,54</sup>

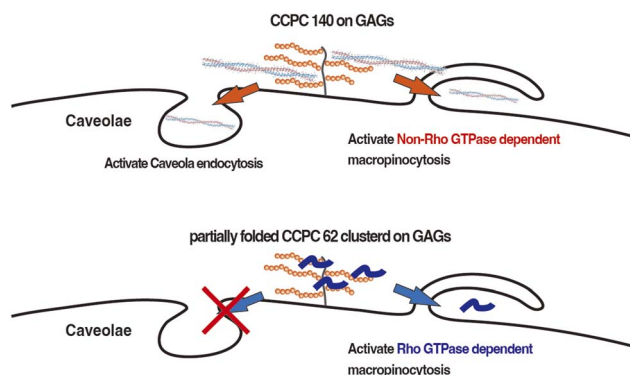


Fig. 6 Schematic illustration of the activation pathways of endocytosis utilized by CCPC 140 and partially folded CCPC 62.

## 4 Conclusions

We previously reported an artificial protein, CCPC 140, which displays superior cellular internalization activity because of its cationic surface properties and rigid and anisotropic structure. The activation of GAG-dependent endocytosis by electrostatic interactions between CCPC 140 and GAGs plays a major role in the superior cellular internalization activity of CCPC 140 and CPPs. Sialic acid itself has an inhibitory effect on the cellular internalization activity, but for unstructured CPPs and partially folded CCPC 62, it may act to recruit CPPs and CCPC 62 to GAGs due to its acidic properties. Macropinocytosis is a common route for the cellular internalization of CCPC 140 and CPPs, but structured CCPCs do not seem to depend on the activation of Rho-family GTPase-induced macropinocytosis. The GAG-binding-dependent activation of caveola-mediated endocytosis plays a role in CCPC 140 cellular internalization. Further studies on biophysical processes will provide important knowledge for the efficient intracellular delivery of pharmaceutical molecules, and control over the activity and endocytic pathways of carriers can be optimized.

## Data availability

All data used in this study were presented in the manuscript. Raw data available upon request to K. S.

## Author contributions

K. S. planned, designed, and performed the experiments, carried out analysis and interpretation of data, and wrote the manuscript. Y. N. assisted in the protein preparation and the cell penetration assay. All authors have given approval to the final version of the manuscript.

## Conflicts of interest

There are no conflicts to declare.

## Acknowledgements

This work was partially supported by a JSPS KAKENHI grant awarded to K.-I. S. (20K05285 and 24K08605), the Network Joint Research Center for Materials, and a special research grant from the Nippon Institute of Technology awarded to K.-I. S. We thank the Edanz Group (<https://www.edanzediting.com/ac>) and MDPI English Editing service for editing this manuscript.

## References

- 1 M. Green and P. M. Loewenstein, Autonomous Functional Domains of Chemically Synthesized Human Immunodeficiency Virus Tat Trans-Activator Protein, *Cell*, 1988, **55**, 1179.
- 2 A. D. Frankel and C. O. Pabo, Cellular Uptake of the Tat Protein from Human Immunodeficiency Virus, *Cell*, 1988, **55**, 1189.



- 3 D. M. Copolovici, K. Langel, E. Eriste and Ü. Langel, Cell-Penetrating Peptides: Design, Synthesis, and Applications, *ACS Nano*, 2014, **8**, 1972.
- 4 M. Zorko and Ü. Langel, Cell-Penetrating Peptides, *Methods Mol. Biol.*, 2022, **2383**, 3.
- 5 P. Agrawal, S. Bhalla, S. S. Usmani, S. Singh, K. Chaudhary, *et al.*, CPPsite 2.0: A Repository of Experimentally Validated Cell Penetrating Peptides, *Nucleic Acids Res.*, 2016, **44**, D1098.
- 6 A. Walrant, S. Cardon, F. Burlina and S. Sagan, Membrane Crossing and Membranotropic Activity of Cell-Penetrating Peptides: Dangerous Liaisons?, *Acc. Chem. Res.*, 2017, **50**, 2968.
- 7 S. Futaki and I. Nakase, Cell-Surface Interactions on Arginine-Rich Cell-Penetrating Peptides Allow for Multiplex Modes of Internalization, *Acc. Chem. Res.*, 2017, **50**, 2449.
- 8 I. Ruseska and A. Zimmer, Internalization Mechanisms of Cell-Penetrating Peptides, *Beilstein J. Nanotechnol.*, 2020, **11**, 101.
- 9 F. Madani, S. Lindberg, Ü. Langel, S. Futaki and A. Gräslund, Mechanisms of Cellular Uptake of Cell-Penetrating Peptides, *J. Biophys.*, 2011, **2011**, 414729.
- 10 M. E. Favretto, R. Wallbrecher, S. Schmidt, R. van de Putte and R. Brock, Glycosaminoglycans in the Cellular Uptake of Drug Delivery Vectors - Bystanders or Active Players?, *J. Contr. Release*, 2014, **180**, 81.
- 11 J. P. Richard, K. Melikov, H. Brooks, P. Prevot, B. Lebleu and L. V. Chernomordik, Cellular Uptake of Unconjugated TAT Peptide Involves Clathrin-Dependent Endocytosis and Heparan Sulfate Receptors, *J. Biol. Chem.*, 2005, **280**, 15300.
- 12 J. M. Gump, R. K. June and S. F. Dowdy, Revised Role of Glycosaminoglycans in TAT Protein Transduction Domain-Mediated Cellular Transduction, *J. Biol. Chem.*, 2010, **285**, 1500.
- 13 I. Nakase, A. Tadokoro, N. Kawabata, T. Takeuchi, H. Katoh, K. Hiramoto, M. Negishi, M. Nomizu, Y. Sugiura and S. Futaki, Interaction of Arginine-Rich Peptides with Membrane-Associated Proteoglycans Is Crucial for Induction of Actin Organization and Macropinocytosis, *Biochemistry*, 2007, **46**, 492.
- 14 H. L. Amand, H. A. Rydberg, L. H. Fornander, P. Lincoln, B. Nordén and E. K. Esbjörner, Cell Surface Binding and Uptake of Arginine- and Lysine-Rich Penetratin Peptides in Absence and Presence of Proteoglycans, *Biochim. Biophys. Acta*, 2012, **1818**, 2669.
- 15 C. Y. Jiao, D. Delaroche, F. Burlina, I. D. Alves, G. Chassaing and S. Sagan, Translocation and Endocytosis for Cell-Penetrating Peptide Internalization, *J. Biol. Chem.*, 2009, **284**, 33957.
- 16 K. Kardani, A. Milani, S. H. Shabani and A. Bolhassani, Cell Penetrating Peptides: The Potent Multi-cargo Intracellular Carriers, *Expert Opin. Drug Deliv.*, 2019, **16**, 1227.
- 17 G. Drin, S. Cottin, E. Blanc, A. R. Rees and J. Tamsamani, Studies on the Internalization Mechanism of Cationic Cell-Penetrating Peptides, *J. Biol. Chem.*, 2003, **278**, 31192.
- 18 I. M. Kaplan, J. S. Wadia and S. F. Dowdy, Cationic TAT Peptide Transduction Domain Enters Cells by Macropinocytosis, *J. Contr. Release*, 2005, **102**, 247.
- 19 I. Nakase, M. Niwa, T. Takeuchi, K. Sonomura, N. Kawabata, Y. Koike, M. Takehashi, S. Tanaka, K. Ueda, J. C. Simpson, A. T. Jones, Y. Sugiura and S. Futaki, Cellular Uptake of Arginine-Rich Peptides: Roles for Macropinocytosis and Actin Rearrangement, *Mol. Ther.*, 2004, **10**, 1011.
- 20 A. Ziegler and J. Seelig, Binding and Clustering of Glycosaminoglycans: a Common Property of Mono- and Multivalent Cell-Penetrating Compounds, *Biophys. J.*, 2008, **94**, 2142.
- 21 K. Donaldson, F. A. Murphy, R. Duffin and C. A. Poland, Asbestos, Carbon Nanotubes and the Pleural Mesothelium: A Review of the Hypothesis regarding the Role of Long Fibre Retention in the Parietal Pleura, Inflammation and Mesothelioma, *Part. Fibre Toxicol.*, 2010, **7**, 5.
- 22 P. N. Yaron, B. D. Holt, P. A. Short, M. Lösche, M. F. Islam and K. N. Dahl, Single Wall Carbon Nanotubes Enter Cells by Endocytosis and Not Membrane Penetration, *J. Nanobiotechnol.*, 2011, **9**, 45.
- 23 J. Du, J. Jin, M. Yan and Y. Lu, Synthetic Nanocarriers for Intracellular Protein Delivery, *Curr. Drug Metab.*, 2012, **13**, 82.
- 24 S. Sharifi, S. Behzadi, S. Laurent, M. L. Forrest, P. Stroeve and M. Mahmoudi, Toxicity of Nanomaterials, *Chem. Soc. Rev.*, 2012, **41**, 2323–2343.
- 25 S. Marchesan, K. Kostarelos, A. Bianco and M. Prato, The Winding Road for Carbon nanotubes in Nanomedicine, *Mater. Today*, 2015, **18**, 12.
- 26 P. M. Costa, M. Bourgoignon, J. T. Wang and K. T. Al-Jamal, Functionalised Carbon Nanotubes: from Intracellular Uptake and Cell-Related Toxicity to Systemic Brain Delivery, *J. Contr. Release*, 2016, **241**, 200.
- 27 N. Nakayama, K. Hagiwara, Y. Ito, K. Ijio, Y. Osada and K. Sano, Superior Cell Penetration by a Rigid and Anisotropic Synthetic Protein, *Langmuir*, 2015, **31**, 2826.
- 28 S. Bienert, A. Waterhouse, T. A. de Beer, G. Tauriello, G. Studer, L. Bordoli and T. Schwede, The SWISS-MODEL Repository-New Features and Functionality, *Nucleic Acids Res.*, 2017, **45**, D313.
- 29 A. Waterhouse, M. Bertoni, S. Bienert, G. Studer, G. Tauriello, R. Gumienny, F. T. Heer, T. A. P. de Beer, C. Rempfer, L. Bordoli, R. Lepore and T. Schwede, SWISS-MODEL: Homology Modelling of Protein Structures and Complexes, *Nucleic Acids Res.*, 2018, **46**, W296.
- 30 F. G. Whitby and G. N. Phillips Jr, Crystal Structure of Tropomyosin at 7 Angstroms Resolution, *Proteins*, 2000, **38**, 49.
- 31 J. Sodek, R. S. Hodges, L. B. Smillie and L. Jurasek, Amino-Acid Sequence of Rabbit Skeletal Tropomyosin and Its Coiled-Coil Structure, *Proc. Natl. Acad. Sci. U. S. A.*, 1972, **69**, 3800.
- 32 A. D. McLachlan and M. Stewart, Tropomyosin Coiled-Coil Interactions: Evidence for an Unstaggered Structure, *J. Mol. Biol.*, 1975, **98**, 293.
- 33 J. Howard, Mechanics of the Cytoskeleton, in *Mechanics of Motor Proteins and the Cytoskeleton*, Sinauer Associates, Inc., Sunderland, MA, 2001, p. 135.



- 34 N. Nakayama, K. Hagiwara, Y. Ito, K. Ijio, Y. Osada and K. Sano, Noncationic Rigid and Anisotropic Coiled-Coil Proteins Exhibit Cell-Penetration Activity, *Langmuir*, 2015, **31**, 8218.
- 35 N. Nakayama, S. Takaoka, M. Ota, K. Takagaki and K. Sano, Effect of the Aspect Ratio of Coiled-Coil Protein Carriers on Cellular Uptake, *Langmuir*, 2018, **34**, 14286.
- 36 R. F. Itzhaki and D. M. Gill, A Micro-biuret Method for Estimating Proteins, *Anal. Biochem.*, 1964, **9**, 401.
- 37 J. D. Esko, T. E. Stewart and W. H. Taylor, Animal Cell Mutants Defective in Glycosaminoglycan Biosynthesis, *Proc. Natl. Acad. Sci. U. S. A.*, 1985, **82**, 3197.
- 38 J. D. Esko, Genetic Analysis of Proteoglycan Structure, Function and Metabolism, *Curr. Opin. Cell Biol.*, 1991, **3**, 805.
- 39 L. K. Hallak, P. L. Collins, W. Knudson and M. E. Peeples, Iduronic Acid-Containing Glycosaminoglycans on Target Cells Are Required for Efficient Respiratory Syncytial Virus Infection, *Virology*, 2000, **271**, 264.
- 40 C. M. Leistner, S. Gruen-Bernhard and D. Glebe, Role of Glycosaminoglycans for Binding and Infection of Hepatitis B Virus, *Cell. Microbiol.*, 2008, **10**, 122.
- 41 T. M. Clausen, D. R. Sandoval, C. B. Spliid, J. Pihl, H. R. Perrett, *et al.*, SARS-CoV-2 Infection Depends on Cellular Heparan Sulfate and ACE2, *Cell*, 2020, **183**, 1043.
- 42 B. Zhou, J. A. Weigel, L. Fauss and P. H. Weigel, Identification of the Hyaluronan Receptor for Endocytosis (HARE), *J. Biol. Chem.*, 2000, **275**, 37733.
- 43 K. G. Rothberg, J. E. Heuser, W. C. Donzell, Y.-S. Ying, J. R. Glenney and R. G. W. Anderson, Caveolin, a protein component of caveolae membrane coats, *Cell*, 1992, **68**, 673–682.
- 44 H. A. Anderson, Y. Chen and L. C. Norkin, Bound Simian Virus 40 Translocates to Caveolin-Enriched Membrane Domains, and Its Entry Is Inhibited by Drugs That Selectively Disrupt Caveolae, *Mol. Biol. Cell*, 1996, **7**, 1825.
- 45 I. Mäger, K. Langel, T. Lehto, E. Eiríksdóttir and Ü. Langel, The Role of Endocytosis on the Uptake Kinetics of Luciferin-Conjugated Cell-Penetrating Peptides, *Biochim. Biophys. Acta*, 2012, **1818**, 502.
- 46 C. K. Payne, S. A. Jones, C. Chen and X. Zhuang, Internalization and Trafficking of Cell Surface Proteoglycans and Proteoglycan-Binding Ligands, *Traffic*, 2007, **8**, 389–401.
- 47 M. R. Bubba, A. M. Senderowicz, E. A. Sausville, K. L. Duncan and E. D. Korn, Jasplakinolide, a Cytotoxic Natural Product, Induces Actin Polymerization and Competitively Inhibits the Binding of Phalloidin to F-Actin, *J. Biol. Chem.*, 1994, **269**, 14869.
- 48 A. S. Desai, M. R. Hunter and A. N. Kapustin, Using Macropinocytosis for Intracellular Delivery of Therapeutic Nucleic Acids to Tumour Cells, *Philos. Trans. R. Soc. Lond. B Biol. Sci.*, 2019, **374**, 20180156.
- 49 P. Sehr, G. Joseph, H. Genth, I. Just and E. Pick, Aktories, Glucosylation and ADP Ribosylation of Rho Proteins: Effects on Nucleotide Binding, GTPase Activity, and Effector Coupling, *Biochemistry*, 1998, **37**, 5296.
- 50 W. P. Ciesla Jr and D. A. Bobak, Clostridium difficile Toxins A and B Are Cation-Dependent UDP-Glucose Hydrolases with Differing Catalytic Activities, *J. Biol. Chem.*, 1998, **273**, 16021.
- 51 S. Gerbal-Chaloin, C. Gondeau, G. Aldrian-Herrada, F. Heitz, C. Gauthier-Rouvière and G. Divita, First Step of the Cell-Penetrating Peptide Mechanism Involves Rac1 GTPase-Dependent Actin-Network Remodelling, *Biol. Cell*, 2007, **99**, 223–238.
- 52 S. Pujals and E. Giralt, Proline-Rich, Amphipathic Cell-Penetrating Peptides, *Adv. Drug Deliv. Rev.*, 2008, **60**, 473.
- 53 J. S. Wadia, R. V. Stan and S. F. Dowdy, Transducible TAT-HA Fusogenic Peptide Enhances Escape of TAT-Fusion Proteins after Lipid Raft Macropinocytosis, *Nat. Med.*, 2004, **10**, 310.
- 54 A. Fittipaldi, A. Ferrari, M. Zoppé, C. Arcangeli, V. Pellegrini, F. Beltram and M. Giacca, Cell Membrane Lipid Rafts Mediate Caveolar Endocytosis of HIV-1 Tat Fusion Proteins, *J. Biol. Chem.*, 2003, **278**, 34141.
- 55 K. L. Veiman, I. Mäger, K. Ezzat, H. Margus, T. Lehto, K. Langel, K. Kurrikoff, P. Arukuusk, J. Suhorutšenko, K. Padari, M. Pooga, T. Lehto and Ü. Langel, PepFect14 Peptide Vector for Efficient Gene Delivery in Cell Cultures, *Mol. Pharm.*, 2013, **10**, 199.

